

Probing Neutrino Oscillation Parameters using High Power Superbeam from ESS

Sanjib Kumar Agarwalla,^a Sandhya Choubey,^{b,c} Suprabh Prakash^b

^a*Institute of Physics, Sachivalaya Marg, Sainik School Post, Bhubaneswar 751005, India*

^b*Harish-Chandra Research Institute, Chhatnag Road, Jhansi, Allahabad 211019, India*

^c*Department of Theoretical Physics, School of Engineering Sciences, KTH Royal Institute of Technology, AlbaNova University Center, 106 91 Stockholm, Sweden*

E-mail: sanjib@iopb.res.in, suprabhprakash@hri.res.in,
sandhya@hri.res.in

ABSTRACT: A high-power neutrino superbeam experiment at the ESS facility has been proposed such that the source-detector distance falls at the second oscillation maximum, giving very good sensitivity towards establishing CP violation. In this work, we explore the comparative physics reach of the experiment in terms of leptonic CP-violation, precision on atmospheric parameters, non-maximal θ_{23} , and its octant for a variety of choices for the baselines. We also vary the neutrino vs. the anti-neutrino running time for the beam, and study its impact on the physics goals of the experiment. We find that for the determination of CP violation, 540 km baseline with 7 years of ν and 3 years of $\bar{\nu}$ ($7\nu + 3\bar{\nu}$) run-plan performs the best and one expects a 5σ sensitivity to CP violation for 48% of true values of δ_{CP} . The projected reach for the 200 km baseline with $7\nu + 3\bar{\nu}$ run-plan is somewhat worse with 5σ sensitivity for 34% of true values of δ_{CP} . On the other hand, for the discovery of a non-maximal θ_{23} and its octant, the 200 km baseline option with $7\nu + 3\bar{\nu}$ run-plan performs significantly better than the other baselines. A 5σ determination of a non-maximal θ_{23} can be made if the true value of $\sin^2 \theta_{23} \lesssim 0.45$ or $\sin^2 \theta_{23} \gtrsim 0.57$. The octant of θ_{23} could be resolved at 5σ if the true value of $\sin^2 \theta_{23} \lesssim 0.43$ or $\gtrsim 0.59$, irrespective of δ_{CP} .

KEYWORDS: Neutrino Oscillation, ESS Facility, Long-baseline, CP Violation, Precision, Octant of θ_{23}

ARXIV EPRINT: [1406.2219](https://arxiv.org/abs/1406.2219)

Contents

1	Introduction and Motivation	1
2	Experimental Specifications	3
3	Oscillation Probability and Simulation Details	4
3.1	θ_{23} -dependence in the disappearance and appearance channels	4
3.2	Numerical procedure	6
4	Results	7
4.1	Discovery of leptonic CP-violation	7
4.2	Precision on atmospheric parameters	9
4.3	Deviation from maximality	10
4.4	Octant resolution	12
5	Summary and Conclusions	16

1 Introduction and Motivation

The current explosion of activity in hunting for signals of physics beyond the Standard Model of particle physics received tremendous boost with the widely confirmed claim that neutrinos have mass [1]. The credit goes to the pioneering world-class experiments involving neutrinos from the Sun [2–8], the Earth’s atmosphere [9, 10], nuclear reactors [11–17], and accelerators [18–23] which have established the phenomenon of neutrino flavor oscillations [24–26] on a strong footing. This immediately demands that neutrinos have mass and they mix with each other, providing an exclusive evidence for physics beyond the Standard Model.

With the recent discovery of the last unknown neutrino mixing angle θ_{13} [13–17, 27], the focus has now shifted towards the determination of the remaining unknown parameters of the three generation neutrino flavor oscillation paradigm. These include the neutrino mass ordering, discovery of CP violation and measurement of the CP phase δ_{CP} in the neutrino sector, and finally determination of the deviation of the mixing angle θ_{23} from maximal and its octant. Various experimental proposals have been put forth to nail these remaining parameters of the neutrino mass matrix. Measurement of non-zero θ_{13} has opened up the chances of determining the neutrino mass ordering, CP violation, as well as the octant of θ_{23} . In particular, the relatively large value of θ_{13} has ensured that the neutrino mass ordering, *aka*, the neutrino mass hierarchy, could be determined to a rather high statistical significance in the next-generation proposed atmospheric [28–33], long-baseline [34–37], and medium-baseline reactor experiments [38, 39]. The determination of the deviation of

θ_{23} from its maximal value and its octant can also be studied in a variety of proposed long-baseline and atmospheric neutrino experiments [40–51]. The chances of exploring CP violation¹ in a given experiment depend on how well one can probe the CP asymmetry A_{CP} which is defined as $(P - \bar{P})/(P + \bar{P})$ where $P(\bar{P})$ are the neutrino (anti-neutrino) probability [56–58]. New experiments with more powerful beams and bigger detectors have been proposed to enhance the CP discovery potential.

There has been a proposal to extend the European Spallation Source (ESS) program to include production of a high intensity neutrino beam, which is being called the European Spallation Source Neutrino Super Beam (ESS ν SB) [59, 60]. Since the neutrino beam is expected to have energies in the few 100s of MeV regime, the proposed detector is a 500 kt MEMPHYS [61, 62] type water Cherenkov detector. The collaboration aims to gain from the R&D already performed for the SPL beam proposed at CERN and the MEMPHYS detector proposed at Frejus. The optimization of the peak beam energy and baseline of the experiment have been studied in [60] in terms of the CP violation discovery reach of this set-up. The choice of peak beam energy of 0.22 GeV and baseline 500 km for this experimental proposal returns a 3σ CP violation discovery potential for almost 70% of $\delta_{CP}(\text{true})$ values [60]. In this paper, we focus on the octant of θ_{23} and its deviation from maximal mixing for a superbeam experiment using a ESS ν SB type beam and MEMPHYS type detector. We will use the ESS ν SB corresponding to 2 GeV protons and consider 500 kt of detector mass for the water Cherenkov far detector and the optimize the experimental set-up taking various possibilities for the baseline of the experiment as well for a different run-time fractions of the beam in the neutrino and anti-neutrino modes.

There remains some tension between the best-fit θ_{23} obtained from the analysis of the MINOS data [63] with the best-fit θ_{23} coming from the analysis of the Super-Kamiokande (SK) atmospheric neutrino data [64], as well as the latest data from the T2K experiment [65]. While the MINOS combined long baseline and atmospheric neutrino data yield the best-fit $\sin^2 \theta_{23} = 0.41(0.61)$ for the lower(higher) octant with a slight preference for the lower octant, SK atmospheric data gives the best-fit at $\sin^2 \theta_{23} = 0.6$ for both normal hierarchy (NH) and inverted hierarchy (IH), and T2K gives the best-fit at $\sin^2 \theta_{23} = 0.514(0.511)$ for NH(IH). The current global fits of the existing world neutrino data by different groups too give conflicting values for the best-fit $\sin^2 \theta_{23}$. While the analysis in [66] gives the best-fit $\sin^2 \theta_{23} = 0.437(0.455)$ for NH(IH), the analysis in [67] gives the best-fit $\sin^2 \theta_{23} = 0.57$ for both NH and IH. In particular, different data sets and different analyses give conflicting answers to the question on whether θ_{23} is maximal. While the preliminary results from T2K indicates near maximal mixing, SK and MINOS data disfavor maximal mixing at slightly over 1σ . On the other hand, the global fits are all inconsistent with maximal θ_{23} at less than 1σ (if we do not assume any knowledge on the mass hierarchy) and have conflicting trends on its octant (irrespective of the hierarchy). Though the tension on the value of θ_{23} and its octant between the different data sets and analyses are not statistically significant, nonetheless they are there, and need to be resolved at the on-going and next-generation

¹For a detailed discussion on the CP violation discovery potential of T2K and NO ν A, see for example [52–55].

neutrino facilities. In addition to determining the value of $\sin^2 2\theta_{23}$, we would also like to determine the θ_{23} octant, in case θ_{23} is found to be indeed non-maximal. The prospects of determining the octant of θ_{23} has been studied before in [40–50] using atmospheric neutrinos and accelerator-based neutrinos beams, and in [68, 69] using reactor neutrinos. We checked that the combined data from present generation long-baseline experiments, T2K and NO ν A can establish a non-maximal θ_{23} only if $\sin^2 \theta_{23}(\text{true}) \lesssim 0.45$ and $\gtrsim 0.57$ at 3σ . The same data can settle the octant of θ_{23} at 2σ provided $\sin^2 \theta_{23}(\text{true}) \lesssim 0.43$ and $\gtrsim 0.58$ irrespective of the value of δ_{CP} [51]. Therefore, it is pertinent to ask whether the next-generation long-baseline experiments can improve these bounds further. Prospects of determining the octant of θ_{23} has been studied in [70–72] for the Long Baseline Neutrino Experiment (LBNE) proposal in the US, and for the Long Baseline Neutrino Oscillation (LBNO) experimental proposal in Europe in [70, 73]. With the help of T2K and NO ν A data, LBNE10 can determine the octant of θ_{23} at 3σ if $\sin^2 \theta_{23}(\text{true}) \lesssim 0.44$ and $\gtrsim 0.59$ for any δ_{CP} [70]. The LBNO proposal with a 10 kt LArTPC can do this job if $\sin^2 \theta_{23}(\text{true}) \lesssim 0.45$ and $\gtrsim 0.58$ [70].

In this work, we study in detail the achievable precision on the atmospheric parameters and the prospects of determining the deviation of θ_{23} from maximal and its correct octant with the ESS ν SB experiment. We consider various baseline and run-plan possibilities for this set-up and optimize them for best reach for θ_{23} octant such that the CP violation discovery reach of the experiment is not significantly compromised. The paper is organized as follows. In section 2, we briefly describe the ESS ν SB proposal from the phenomenological viewpoint. In section 3, we give the details of the simulation procedure. In section 4, we describe the results we obtain regarding the sensitivities of the ESS ν SB set-up. Finally, in section 5, we give our conclusions.

2 Experimental Specifications

In this section we briefly describe the super beam set-up that we have considered in this study. The ESS project is envisaged as a major European facility providing slow neutrons for research as well as the industry. It is projected to start operation by 2019. The ESS ν SB proposal is an extension of the original ESS facility to generate an intense neutrino beam for neutrino oscillation studies. The proposal is to use the 5 MW ESS proton driver with 2 GeV protons, to produce a high intensity neutrino superbeam simultaneously along with the spallation neutrons, without compromising on the number of spallation neutrons. This dual purpose machine would result in considerable reduction of costs in contrast to the building of two separate proton drivers, one for neutrons and another for neutrinos. The proton driver could later be used as a part of the neutrino factory, if and when one is built. Detailed feasibility studies for this dual purpose machine is underway. We refer the readers to [60] for a detailed discussion on the accelerator, target station and the beam line being discussed for this proposal. While the proposed proton energy for the ESS facility is 2 GeV, the energy of the protons could be increased up to 3 GeV. The expected neutrino flux for this facility has been calculated for proton energy of 2 GeV and 2.7×10^{23} protons on target per year, corresponding to 5 MW power for the beam. For the other proton

energies of 2.5 GeV and 3 GeV, the neutrino flux is calculated by keeping the power of the beam fixed at 5 MW. In this paper, we use the neutrino fluxes corresponding to the 2 GeV proton beam and 2.7×10^{23} protons on target per year [60].

The on-axis neutrino flux for the 2 GeV protons on target peaks at 0.22 GeV. Hence, megaton class water Cherenkov detector has been proposed as the default detector option for this set-up. At these energies, the detection cross-section is dominated by quasi-elastic scattering. We have used the GLOBES software [74, 75] to simulate the ESS ν SB set-up. We obtain the fluxes from [76] and consider the properties of the MEMPHYS detector [61, 77] to simulate the events. We take the fiducial mass of the detector to be 500 kt and a total run-time of 10 years.

For the peak neutrino energy of 0.22 GeV obtained for the 2 GeV protons on target, the first oscillation maximum corresponds to 180 km while the second oscillation maximum comes at 540 km. The possible detector locations are discussed in [60]. Existing mines in Sweden where the detector can be housed are at distances of about 260 km (Oskarshamn), 360 km (Zinkgruvan), 540 km (Garpenberg) and 1090 km (Kristineberg) from the ESS site, which is in Lund. The study in [60] uses the mine location at Garpenberg to place the detector, giving a baseline of 540 km which corresponds to the second oscillation maximum, well suited for CP violation discovery [78]. The study shows that the CP violation discovery can be achieved for up to 50% values of $\delta_{\text{CP}}(\text{true})$ at more than 5σ . In what follows, we optimize the baseline for the deviation of θ_{23} from maximal and its octant, without severely compromising the sensitivity to CP violation. The number of events that we get for the set-up described above is shown in Table 1. It can be seen that event numbers in Table 1 have a good match with Table 3 of [60].

Set-up	$\nu_e(\bar{\nu}_e)$ signal	$\nu_\mu(\bar{\nu}_\mu)$ miss-ID	ν_e intrinsic	$\bar{\nu}_e$ intrinsic	NC	$\bar{\nu}_\mu(\nu_\mu) \rightarrow \bar{\nu}_e(\nu_e)$ wrong-sign contamination
360 km (ν run)	304	10	75	0.08	25	1.0
($\bar{\nu}$ run)	244	6	3	53	15	11
540 km (ν run)	197	5	34	0.04	11	0.7
($\bar{\nu}$ run)	164	3	1	24	7	7

Table 1: Signal and background events for the ESS ν SB set-up with a 360 km baseline and a 540 km baseline. Both ν and $\bar{\nu}$ events are shown. To generate these numbers, we used the following values of the neutrino oscillation parameters: $\Delta m_{21}^2 = 7.5 \times 10^{-5} \text{eV}^2$, $\Delta m_{31}^2 = 2.47 \times 10^{-5} \text{eV}^2$, $\sin^2 \theta_{12} = 0.3$, $\sin^2 2\theta_{13} = 0.087$, $\sin^2 \theta_{23} = 0.415$ and $\delta_{\text{CP}} = 0$. These values are the same as that used to generate Table 3 of [60].

3 Oscillation Probability and Simulation Details

Here, we focus on the relevant oscillation channels and simulation methods which go in estimating the final results.

3.1 θ_{23} -dependence in the disappearance and appearance channels

The precision measurement of the mixing angle θ_{23} in long-baseline experiments comes from the disappearance channel. This channel depends on the survival probability for

muon neutrinos, which in the approximation that $\Delta m_{21}^2 = 0$ is given as [44]

$$\begin{aligned}
P(\nu_\mu \rightarrow \nu_\mu) \approx & 1 - \sin^2 \theta_{13}^M \sin^2 2\theta_{23} \sin^2 \frac{[(\Delta m_{31}^2 + A) - (\Delta m_{31}^2)^M]L}{8E} \\
& - \cos^2 \theta_{13}^M \sin^2 2\theta_{23} \sin^2 \frac{[(\Delta m_{31}^2 + A) + (\Delta m_{31}^2)^M]L}{8E} \\
& - \sin^2 2\theta_{13}^M \sin^4 \theta_{23} \sin^2 \frac{(\Delta m_{31}^2)^M L}{4E}, \tag{3.1}
\end{aligned}$$

where θ_{13}^M and $(\Delta m_{31}^2)^M$ are the mixing angle θ_{13} and Δm_{31}^2 in matter and A is the Wolfenstein matter term [79] and is given by $A(\text{eV}^2) = 0.76 \times 10^{-4} \rho (\text{g/cm}^3) E(\text{GeV})$. The disappearance data through its sensitivity to $\sin^2 2\theta_{23}$ as seen in the leading first term in Eq. (3.1) provides stringent constraint. This provides a powerful tool for testing a maximal θ_{23} against a non-maximal one. However, the leading first term does not depend on the octant of θ_{23} . This dependence comes only at the sub-leading level from the third term in Eq. (3.1), which becomes relevant only when matter effects are very large to push $\sin^2 \theta_{13}^M$ close to resonance. Since the ESS ν SB set-up involves very low neutrino energies and short baselines, the disappearance channel would provide almost no octant sensitivity and if θ_{23} was indeed non-maximal, it would give narrow allowed-regions in both the lower and the higher octant of θ_{23} .

The octant sensitivity of long baseline experiments come predominantly from the electron appearance channel which depends on the $P(\nu_\mu \rightarrow \nu_e)$ transition probability. Since this channel also gives sensitivity to CP violation for non-zero Δm_{21}^2 , we give here the $\nu_\mu \rightarrow \nu_e$ oscillation probability in matter, expanded perturbatively in $\alpha (= \Delta m_{21}^2 / \Delta m_{31}^2)$ and $\sin \theta_{13}$, keeping up to the second order terms in these small parameters [80–82]

$$\begin{aligned}
P(\nu_\mu \rightarrow \nu_e) \sim P_{\mu e} = & \sin^2 2\theta_{13} \sin^2 \theta_{23} \frac{\sin^2 \hat{\Delta}(1 - \hat{A})}{(1 - \hat{A})^2} \\
& + \alpha \cos \theta_{13} \sin 2\theta_{12} \sin 2\theta_{13} \sin 2\theta_{23} \cos(\hat{\Delta} + \delta_{\text{CP}}) \frac{\sin \hat{\Delta} \hat{A} \sin \hat{\Delta}(1 - \hat{A})}{\hat{A} (1 - \hat{A})} \\
& + \alpha^2 \sin^2 2\theta_{12} \cos^2 \theta_{13} \cos^2 \theta_{23} \frac{\sin^2 \hat{\Delta} \hat{A}}{\hat{A}^2} \tag{3.2}
\end{aligned}$$

where $\hat{\Delta} = \Delta m_{31}^2 L / 4E$ and $\hat{A} = A / \Delta m_{31}^2$ are dimensionless parameters. The leading first term in Eq. (3.2) depends on the octant of θ_{23} . Octant dependence comes also from the third term, however this term is suppressed at second order in α . The δ_{CP} dependence comes only in the second term which goes as $\sin 2\theta_{23}$. However, it was shown in [51] that the presence of the δ_{CP} term in the probability brings in a $\delta_{\text{CP}} - \theta_{23}$ degeneracy which can be alleviated only through a balanced run of the experiment between the neutrino and anti-neutrino channels.

The approximate expressions in this section is given only for illustration. Our numerical analysis is done using the full three-generation oscillation probabilities. For the analysis performed in this paper, we simulate predicted events at the following true values of the oscillation parameters: $\sin^2 2\theta_{13} = 0.089$, $\Delta m_{21}^2 = 7.5 \times 10^{-5} \text{ eV}^2$, $\sin^2 \theta_{12} = 0.3$, while the values for θ_{23} and δ_{CP} are varied within their allowed ranges. We take the true value of

atmospheric splitting to be $\Delta m_{\mu\mu}^2 = \pm 2.4 \times 10^{-3} \text{ eV}^2$ where +ve (-ve) sign is for NH (IH). The relation between $\Delta m_{\mu\mu}^2$ and Δm_{31}^2 has been taken from [83, 84]. Our assumptions for the systematic uncertainties considered are as follows. For the appearance channel, we take 10% signal normalization error and 25% background normalization error. For the disappearance events, we take 5% signal normalization error and 10% background normalization error. For both types of events, a 0.01% energy calibration error has been assumed. These ‘simulated events’ is then fitted by means of a χ^2 to determine the sensitivity of the experiment to the different performance indicators. We use the following definition of χ^2 :

$$\chi^2 = \min_{\xi_s, \xi_b} \left[2 \sum_{i=1}^n (\tilde{y}_i - x_i - x_i \ln \frac{\tilde{y}_i}{x_i}) + \xi_s^2 + \xi_b^2 \right], \quad (3.3)$$

where n is the total number of bins and

$$\tilde{y}_i(\{\omega\}, \{\xi_s, \xi_b\}) = N_i^{th}(\{\omega\}) [1 + \pi^s \xi_s] + N_i^b [1 + \pi^b \xi_b]. \quad (3.4)$$

Above, $N_i^{th}(\{\omega\})$ is the predicted number of events in the i -th energy bin for a set of oscillation parameters ω and N_i^b are the number of background events in bin i . The quantities π^s and π^b in Eq. 3.4 are the systematical errors on signals and backgrounds respectively. The quantities ξ_s and ξ_b are the pulls due to the systematical error on signal and background respectively. x_i is the predicted event rates corresponding to the i -th energy bin, consisting of signal and backgrounds. χ^2 corresponding to all the channels defined in the experiment are calculated and summed over. Measurements of oscillation parameters available from other experiments are incorporated through Gaussian priors.

$$\chi_{\text{total}}^2 = \sum_{j=1}^c \chi_j^2 + \chi_{\text{prior}}^2 \quad (3.5)$$

where c is the total number of channels. Finally, χ_{total}^2 is marginalized in the fit over the allowed ranges in the oscillation parameters to find $\Delta\chi_{\text{min}}^2$. More details of χ^2 definition, as given in Eqs. 3.3 and 3.4, can be found in [85, 86].

3.2 Numerical procedure

Leptonic CP-violation: To evaluate the sensitivity to leptonic CP-violation, we follow the following approach. We first assume a true value of δ_{CP} lying in the allowed range of $[-180^\circ, 180^\circ]$. The event spectrum assuming this true δ_{CP} is calculated and is labeled as *predicted* event spectra. We then calculate the various *theoretical* event spectra assuming the test δ_{CP} to be the CP-conserving values 0 or π and by varying the other oscillation parameters in their $\pm 2\sigma$ range (the solar parameters are not varied) except θ_{23} which is varied in the $\pm 3\sigma$ range. We add prior on $\sin^2 2\theta_{13}$ ($\sigma = 5\%$) as expected after the full run of Daya Bay [87]. We use the software GLoBES to calculate the $\Delta\chi^2$ between each set of predicted and theoretical events. The smallest of all such $\Delta\chi^2$: $\Delta\chi_{\text{min}}^2$ is considered. The results are shown by plotting $\Delta\chi_{\text{min}}^2$ as a function of assumed true value in the range $[-180^\circ, 180^\circ]$.

Precision on $\Delta m_{\mu\mu}^2$ and $\sin^2 \theta_{23}$: We simulate the *predicted* events due to a true value of $\Delta m_{\mu\mu}^2$. For generating the *theoretical* spectrum, values of $\Delta m_{\mu\mu}^2$ in the $\pm 2\sigma$ range around the central true value are chosen. We marginalize over rest of the oscillation parameters including hierarchy in order to calculate the $\Delta\chi_{\min}^2$. Similar procedure is followed in the case of $\sin^2 \theta_{23}$, with the exception that for non-maximal true values of θ_{23} , we confine the test range to be in the true octant only.

Sensitivity to maximal vs. non-maximal θ_{23} : We consider true $\sin^2 \theta_{23}$ values in the allowed 3σ range and calculate events, thus simulating the true events. This is then contrasted with *theoretical* event spectra assuming the test $\sin^2 \theta_{23}$ to be 0.5. Rest of the oscillation parameters, including hierarchy, are marginalized to obtain the least $\Delta\chi^2$. This procedure is done for a fixed true δ_{CP} value of 0 and normal mass hierarchy.

Sensitivity to Octant of θ_{23} : To calculate the sensitivity to the octant of θ_{23} , the following approach is taken. We take a true value of $\sin^2 \theta_{23}$ lying in the lower octant. The other known oscillation parameters are kept at their best-fit values. Various test $\sin^2 \theta_{23}$ values are taken in the higher octant. Test values for other oscillation parameters are varied in the $\pm 2\sigma$ range. We marginalize over the hierarchies. $\Delta\chi^2$ values between the true and test cases are calculated and the least of all such values: $\Delta\chi_{\min}^2$ is considered. This is repeated for a true $\sin^2 \theta_{23}$ lying in the higher octant, but this time the test values of $\sin^2 \theta_{23}$ are considered from the lower octant only. This is done for both NH and IH as true choice and various values of $\delta_{\text{CP}}(\text{true})$ in $[-180^\circ, 180^\circ]$.

4 Results

In this section, we report our findings regarding the leptonic CP-violation, achievable precision on atmospheric parameters, non-maximality of θ_{23} and its octant for the proposed ESS ν SB set-up.

4.1 Discovery of leptonic CP-violation

We first show the results for the sensitivity of the ESS ν SB set-up to CP violation. We compare the sensitivity of the set-up for different possible baseline options. We have chosen the representative values of 200 km, 360 km, 540 km and 800 km which are the same as what has been considered in [60]. In Fig. 1, we show the discovery reach towards CP violation for these prospective baselines.² In the y-axis, we have plotted the confidence level (C.L.), (defined as $\sqrt{\Delta\chi_{\min}^2}$) and in the x-axis we have plotted the true δ_{CP} values lying in the range $[-180^\circ, 180^\circ]$. The left panel is assuming the NH to be the true hierarchy while, in the right panel we have assumed IH to be the true hierarchy. The run plan considered here is two years of neutrino running followed by eight years of anti-neutrino running ($2\nu + 8\bar{\nu}$), to match with the run plan assumed in the ESS ν SB proposal [60]. In producing these plots, we have considered the test hierarchy to be the same as the true one which implies that we have not marginalized over hierarchies while calculating the $\Delta\chi^2$. Note that the

²It should be noted that for producing the results for CP violation, the values of true oscillation parameters considered are the same as those in Table 1. While, these values are the same as those considered in [60], they are different from what we have taken for producing other results in this paper.

CP discovery reach results shown in [60] are obtained after marginalizing over the neutrino mass hierarchy. We have performed our analysis for the CP discovery reach both with and without marginalizing over the mass hierarchy and have presented the results for the fixed test hierarchy case. The underlying justification for doing this is the fact that by the time this experiment comes up, we may have a better understanding of the neutrino mass hierarchy. In addition, from the observation of atmospheric neutrino events in the 500 kt water Cherenkov detector deployed for the ESS ν SB set-up, 3σ to 6σ sensitivity to the mass hierarchy is expected, depending on the true value of $\sin^2 \theta_{23}$. Here one assumes that the ESS ν SB far detector will have similar features to the Hyper-Kamiokande proposal in Japan [88]. The impact of marginalization over the hierarchy is mainly in reducing somewhat the CP coverage for the $L = 200$ km baseline option. For the other baselines, the impact of marginalizing over the test hierarchy is lower mainly because for these longer baselines the hierarchy degeneracy gets resolved via the ESS ν SB set-up alone.

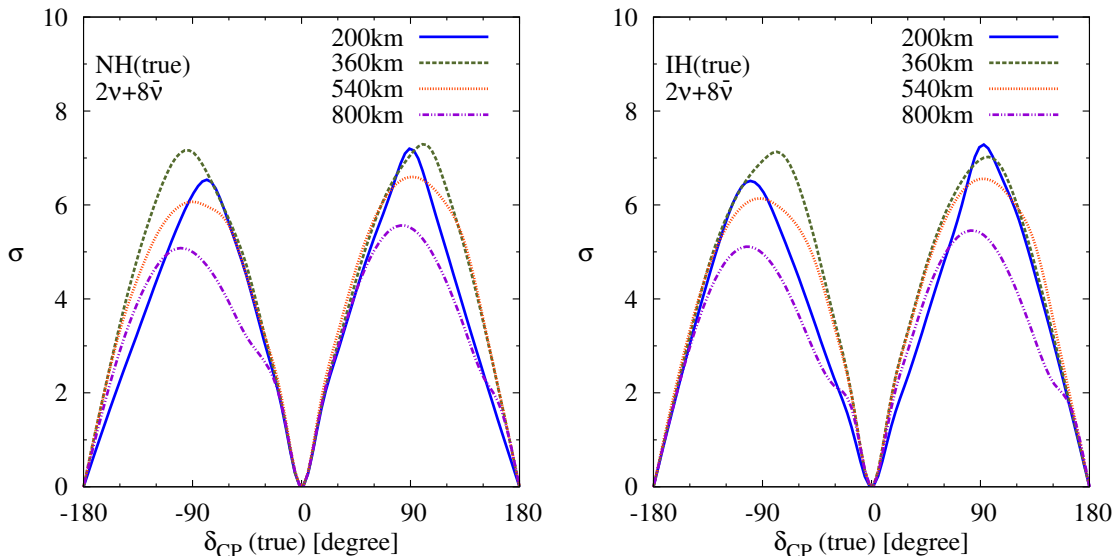


Figure 1: CP violation discovery potential (in σ) as a function of $\delta_{\text{CP}}(\text{true})$. The left(right) panel assumes NH(IH) to be the true hierarchy. Baselines corresponding to 200 km, 360 km, 540 km and 800 km have been considered. The choice of run-plan is $2\nu + 8\bar{\nu}$ years of running.

Fig. 1 shows that our results for CP violation are in agreement with those in [60]. From the left panel of Fig. 1, it can be seen that for the 200 km baseline, which is the smallest amongst the four choices considered, a 3σ C.L. evidence of CP violation is possible for 60% of $\delta_{\text{CP}}(\text{true})$, while a 32% coverage is possible at 5σ C.L. For the 540 km baseline, which shows the best sensitivities amongst the four choices considered, discovery of CP violation at the 3σ C.L. is expected to be possible for 70% of $\delta_{\text{CP}}(\text{true})$, while a 5σ significance is expected for 45% of $\delta_{\text{CP}}(\text{true})$. Thus, we are led to the conclusion that the 540 km choice is better-suited for the discovery of CP-violation with this set-up than any other choice of baseline. However, the CP violation discovery reach of the 360 km and 200 km baselines are only marginally lower. In particular, we note that if we have to change from the 540 km baseline to 200 km baseline, the CP coverage for CP violation discovery goes down

only by $\sim 13\%$ (10%) at the 5σ (3σ) C.L.

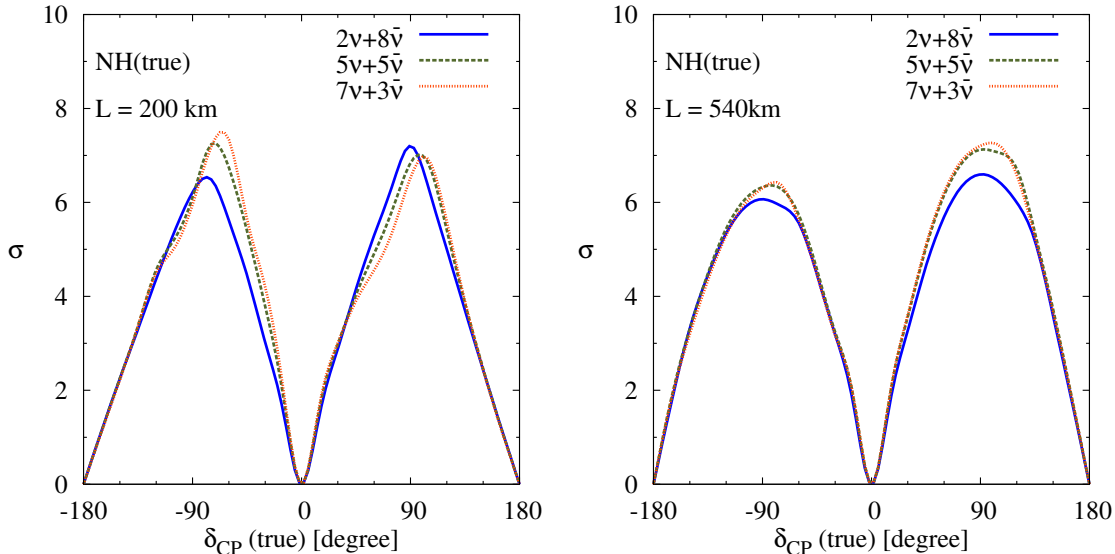


Figure 2: Statistical significance (σ) for CP violation discovery potential as a function of $\delta_{\text{CP}}(\text{true})$. NH has been assumed to be the true hierarchy. The left(right) panel corresponds to the choice of 200 km (540 km) as the baseline. Results for different run-plans corresponding to $2\nu + 8\bar{\nu}$, $5\nu + 5\bar{\nu}$ and $7\nu + 3\bar{\nu}$ years of running have been shown.

In [60], the nominal choice for the neutrino vs. anti-neutrino run-plan for the ESS ν SB was taken as $2\nu + 8\bar{\nu}$. The motivation behind this choice was to have similar number of events for both ν and $\bar{\nu}$ running. However, in order to explore this further, we calculate the sensitivity to CP violation for different run-plans. We have taken three cases: $2\nu + 8\bar{\nu}$, $5\nu + 5\bar{\nu}$, and $7\nu + 3\bar{\nu}$. The left (right) panel in Fig. 2 shows the projected CP discovery potential for the 200 km (540 km) baseline option, for different run-plans. From these plots, it can be seen that at lower C.L., all the three run-plans have similar sensitivity. However, at 5σ C.L., the larger coverage in δ_{CP} comes with $7\nu + 3\bar{\nu}$ running. While this holds true for both 200 km and 540 km, the effect is marginally more pronounced for the 200 km baseline option.

4.2 Precision on atmospheric parameters

We now focus on the achievable precision on atmospheric parameters with the proposed set-up. The precision³ is mainly governed by the $P(\nu_{\mu} \rightarrow \nu_{\mu})$ channel (see Eq. (3.1)). Because of huge statistics in this channel, we expect this set-up to pin down the atmospheric parameters to ultra-high precision. Indeed, this is the case as can be seen from Table 2. Table 2 shows the relative 1σ precision on $\Delta m_{\mu\mu}^2$ and $\sin^2 \theta_{23}$ considering three different values of true $\sin^2 \theta_{23}$. Here, we have taken the baseline to be 200 km and the run-plan to be $7\nu + 3\bar{\nu}$.

It can be seen that around 0.2% precision on the atmospheric mass splitting is achievable which is a factor of ~ 5 better than what can be achieved with combined data from

³We define the relative 1σ error as 1/6th of the $\pm 3\sigma$ variations around the true choice.

$\sin^2 \theta_{23}(\text{true})$	0.4	0.5	0.6
$\delta(\Delta m_{\mu\mu}^2)$	0.24%	0.2%	0.22%
$\delta(\sin^2 \theta_{23})$	1.12%	3.0%	0.8%

Table 2: Relative 1σ precision (1 dof) on $\Delta m_{\mu\mu}^2$ and $\sin^2 \theta_{23}$ considering three different values of true $\sin^2 \theta_{23}$. Here, for all the cases, we consider the true value of $\Delta m_{\mu\mu}^2$ to be $2.4 \times 10^{-3} \text{eV}^2$. We consider NH as the true hierarchy. We have considered the 200 km as the baseline and $7\nu + 3\bar{\nu}$ as the run-plan for generating these numbers.

T2K and NO ν A [89]. While the precision on $\Delta m_{\mu\mu}^2$ is weakly-dependent on the true value of $\sin^2 \theta_{23}$, the precision in $\sin^2 \theta_{23}$ shows a large dependence on its central value. We see that for $\sin^2 \theta_{23} = 0.5$, the precision is 3.0%, while for $\sin^2 \theta_{23} = 0.6$, its 0.8%. The precision in $\sin^2 \theta_{23}$ is worst for the maximal mixing due to the fact that a large Jacobian is associated with transformation of the variable from $\sin^2 2\theta_{23}$ to $\sin^2 \theta_{23}$ around the maximal mixing [41].

4.3 Deviation from maximality

As discussed in the Introduction, currently different data sets have a conflict regarding the best-fit value of θ_{23} and its deviation from maximal mixing. While global analysis of all data hint at best-fit θ_{23} being non-maximal, these inferences depend on the assumed true mass hierarchy and are also not statistically very significant. Therefore, these results would need further corroboration in the next-generation experiments. If the deviation of θ_{23} from maximal mixing is indeed small, it may be difficult for the present generation experiment to establish a deviation from maximality. It has been checked that the combined results from T2K and NO ν A will be able to distinguish a non-maximal value of θ_{23} from the maximal value $\pi/4$ at 3σ C.L. if $\sin^2 \theta_{23}(\text{true}) \lesssim 0.45$ and $\gtrsim 0.57$. In such a situation, it will be interesting to know how well the ESS ν SB set-up can establish a non-maximal $\sin^2 \theta_{23}$. In Fig. 3, we show the sensitivity of various baselines towards establishing a non-maximal $\sin^2 \theta_{23}$. These plots show the $\Delta\chi^2$ as a function of the true $\sin^2 \theta_{23}$, where $\Delta\chi^2$ is as defined in section 3.

The results are shown for the prospective baselines of 200 km, 360 km, 540 km and 800 km. The top left (right) panel corresponds to the choice of δ_{CP} (true) of 0 (90°). The bottom left (right) panel corresponds to the choice of true δ_{CP} of -90° (180°). The true hierarchy for all these plots is assumed to be NH and the run-plan is taken to be $7\nu + 3\bar{\nu}$. Here, we have marginalized the $\Delta\chi^2$ over the hierarchy. It can be seen from Fig. 3 that the best sensitivity occurs for the 200 km baseline. For true $\delta_{\text{CP}} = 0$, a 3σ determination of non-maximal $\sin^2 2\theta_{23}$ can be made if $\sin^2 \theta_{23} \lesssim 0.47$ or if $\sin^2 \theta_{23} \gtrsim 0.56$. A 5σ determination is possible if $\sin^2 \theta_{23} \lesssim 0.45$ or if $\sin^2 \theta_{23} \gtrsim 0.57$. We checked that the contribution to the sensitivity from the appearance channels is small compared to that from the disappearance channels. This is reflected in the fact that there is a small dependence of $\Delta\chi^2$ on the assumed true value of δ_{CP} . An interesting observation is that the $\Delta\chi^2$ curve is not symmetric around the $\sin^2 \theta_{23} = 0.5$ line. It seems that, as far as observing a deviation from maximality is concerned, the lower octant is more favored than the higher octant. The reason behind this feature is the following. The sensitivity here, is

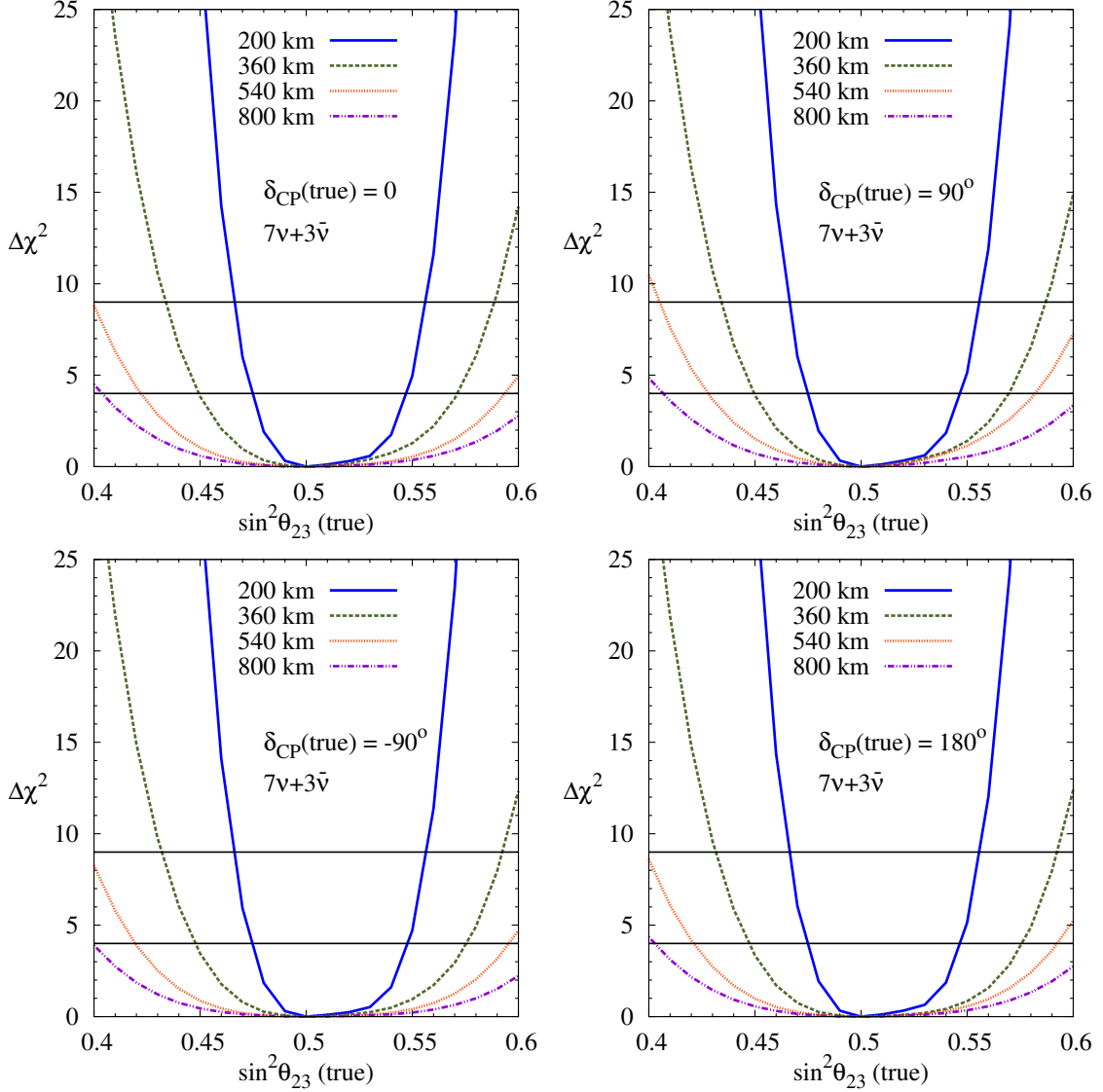


Figure 3: $\Delta\chi^2_{\min}$ for a non-maximal θ_{23} discovery vs. $\sin^2\theta_{23}(\text{true})$ for the ESS ν SB set-up. NH has been assumed to be the true hierarchy and the choice of run-plan has been taken to be $7\nu + 3\bar{\nu}$ years of running. Results corresponding to various choices: 200 km, 360 km, 540 km and 800 km for the baseline have been shown. The top-left/top-right/bottom-left/bottom-right panel corresponds to $0/90^\circ/-90^\circ/180^\circ$ assumed as $\delta_{\text{CP}}(\text{true})$. The horizontal black lines show 2σ and 3σ confidence level values.

mostly governed by the disappearance data in which the measured quantity is $\sin^2 2\theta_{\mu\mu}$. Since $\sin^2\theta_{23} = \sin^2\theta_{\mu\mu}/\cos^2\theta_{13}$ [83, 84, 90], the θ_{13} correction shifts the θ_{23} values towards 45° in the lower octant and away from 45° in the higher octant. This results in the shifting of the curve towards the right in $\sin^2\theta_{23}$ and is reflected as the asymmetric nature of the curve. We have checked that for the (now) academic case of $\theta_{13}(\text{true})=0$, the $\Delta\chi^2$ curve is symmetric around 45° .

To find an optimal run-plan in the case of deviation from maximality, we generated the results for 200 km baseline for ESS ν SB set-up, assuming NH and $\delta_{\text{CP}} = 0$. Three run-plans

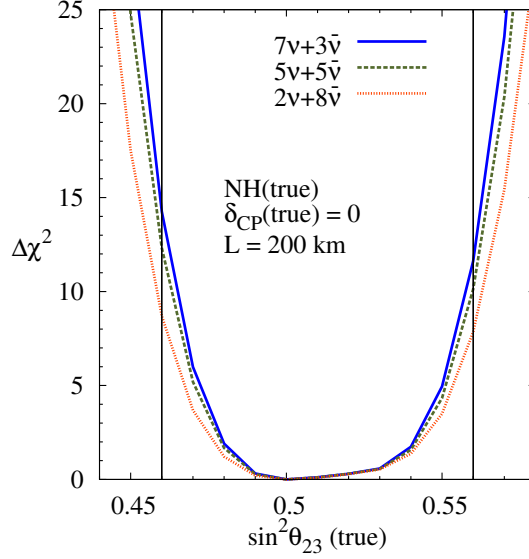


Figure 4: $\Delta\chi^2_{\min}$ for a non-maximal θ_{23} discovery vs. $\sin^2\theta_{23}$ (true) for the ESS ν SB set-up. NH has been assumed to be the true hierarchy and $\delta_{\text{CP}}(\text{true})$ has been assumed to be 0. The choice of baseline has been taken to be 200 km. Results corresponding to various choices: $2\nu + 8\bar{\nu}$, $5\nu + 5\bar{\nu}$ and $7\nu + 3\bar{\nu}$ years of running for the run-plan have been shown. The purpose of having vertical lines at $\sin^2\theta_{23}$ true = 0.46 and 0.56 is to show the effect of run-plan on sensitivity (see Table 3 for discussion on this).

were assumed as before: $2\nu + 8\bar{\nu}$, $5\nu + 5\bar{\nu}$ and $7\nu + 3\bar{\nu}$. It can be seen from Fig. 4 that the best results are observed for $7\nu + 3\bar{\nu}$. Thus, this run-plan seems to be optimally suited for measurement of deviation from maximality as well. Note that apparently it seems from Fig. 4 that the sensitivity in the case of different run-plans are roughly the same despite there being huge change of statistics in terms of neutrino and anti-neutrino data. However, a closer look will reveal that the $\Delta\chi^2$ indeed changes as expected with the increase in the total statistics collected by the experiment and in fact it is the very sharp rise of the curves which hides the difference. To illustrate this further, we show in Table 3 the $\Delta\chi^2$ values corresponding to different run-plans at different true $\sin^2\theta_{23}$ values and for two choices of $\sin^2\theta_{23}(\text{true})$.

$\sin^2\theta_{23}$ (true)	$2\nu + 8\bar{\nu}$	$5\nu + 5\bar{\nu}$	$7\nu + 3\bar{\nu}$
0.46	8.7	12.3	14.2
0.56	7.8	10.1	11.6

Table 3: $\Delta\chi^2_{\min}$ for $\sin^2\theta_{23}$ (true) = 0.46 and 0.56. Here, the sensitivity of the ESS ν SB set-up to the deviation from a maximal θ_{23} has been considered. NH has been assumed to be the true hierarchy and $\delta_{\text{CP}}(\text{true})$ has been assumed to be 0. The choice of baseline has been taken to be 200 km. Results corresponding to various choices: $2\nu + 8\bar{\nu}$, $5\nu + 5\bar{\nu}$ and $7\nu + 3\bar{\nu}$ years of running for the run-plan have been shown in different columns.

4.4 Octant resolution

In this section, we explore the octant resolving capability of the ESS ν SB set-up. As discussed in the previous section, we generate true event rates at certain $\sin^2\theta_{23}(\text{true})$ and

fit this by marginalizing over the entire $\sin^2 \theta_{23}$ range in the wrong octant. The $\Delta\chi^2$ is also marginalized over $|\Delta m_{31}^2|$, $\sin^2 \theta_{13}$, δ_{CP} and the neutrino mass hierarchy. Fig. 5 shows the $\Delta\chi^2$ obtained as a function of $\sin^2 \theta_{23}(\text{true})$ assuming NH to the true hierarchy. The corresponding results for the IH(true) case is shown in Fig. 6. We show the results for 200 km, 360 km, 540 km, and 800 km baselines in the first, second, third, and fourth rows respectively. The first column corresponds to the $2\nu + 8\bar{\nu}$ run-plan. The second column corresponds to the $5\nu + 5\bar{\nu}$ run-plan while the third column corresponds to the $7\nu + 3\bar{\nu}$ run-plan. The band in each of these plots correspond to variation of $\delta_{\text{CP}}(\text{true})$ in the range $[-180^\circ, 180^\circ]$. Thus, for any $\sin^2 \theta_{23}(\text{true})$, the top-most and the bottom-most $\Delta\chi^2$ values lying in the band shows the maximum and minimum $\Delta\chi^2$ possible depending on the true value of δ_{CP} .

From the plots in Fig. 5 and Fig. 6, it can be seen that the best choice for θ_{23} octant resolution seems to be the 200 km baseline. Since amongst the various choices, the 200 km baseline is the closest to the source, it has the largest statistics for both ν and $\bar{\nu}$ samples. This is the main reason why the 200 km option returns the best octant resolution prospects. We have explicitly checked that if the statistics of the the other baseline options were scaled to match the one we get for the 200 km baseline option, they would give θ_{23} octant sensitivity close to that obtained for the 200 km option. We can also see from these figures that the best sensitivity is expected for the run-plan of $7\nu + 3\bar{\nu}$. Note also that the $5\nu + 5\bar{\nu}$ run-plan is just marginally worse than the $7\nu + 3\bar{\nu}$ plan. However, these two run-plans are better than $2\nu + 8\bar{\nu}$ run-plan. This again comes because of the fact that this option allows for larger statistics while maintaining a balance between the ν and $\bar{\nu}$ data, which is required to cancel degeneracies for maximum octant resolution capability as was shown in [51]. The impact of the run plans are again seen to be larger for the larger baselines. We can also see that the impact of $\delta_{\text{CP}}(\text{true})$ is larger for larger baselines. The δ_{CP} band is narrowest for the 200 km baseline option, implying that this baseline choice suffers least uncertainty from unknown $\delta_{\text{CP}}(\text{true})$ for octant studies.

Assuming NH(true) and with the 200 km baseline and $7\nu + 3\bar{\nu}$ run-plan option, one can expect to resolve the correct octant of θ_{23} at the 3σ level for $\sin^2 \theta_{23}(\text{true}) \lesssim 0.43$ and $\gtrsim 0.59$ irrespective of $\delta_{\text{CP}}(\text{true})$. Correct octant can be identified with this option at 5σ confidence level for $\sin^2 \theta_{23}(\text{true}) \lesssim 0.37$ and $\gtrsim 0.63$ for all values of $\delta_{\text{CP}}(\text{true})$. For IH(true) the corresponding values for 3σ (5σ) sensitivity are $\sin^2 \theta_{23}(\text{true}) \lesssim 0.43(0.37)$ and $\gtrsim 0.59(0.62)$. These numbers and a comparison of Fig. 5 and 6 reveals that the octant sensitivity of the ESS ν SB set-up does not depend much on the assumed true mass hierarchy. The octant sensitivity for both true hierarchies and all run-plan options is seen to deteriorate rapidly with the increase in the baseline. For the 540 km baseline option, we find that even for $\sin^2 \theta_{23}(\text{true}) > 0.35$ and < 0.63 , we do not get a 3σ resolution of the octant for 100% values of $\delta_{\text{CP}}(\text{true})$.

To show the impact of $\delta_{\text{CP}}(\text{true})$ on the determination of the octant of θ_{23} at ESS ν SB, we show in Fig. 7 the 3σ contours in the $\sin^2 \theta_{23}(\text{true})$ - $\delta_{\text{CP}}(\text{true})$ plane for different baselines. We assume the $7\nu + 3\bar{\nu}$ run-plan for this figure. The left hand panel shows the contours for NH(true) while the right hand panel is for IH(true). The different lines show the contours for the different baselines. Comparison of the different lines reveals that the

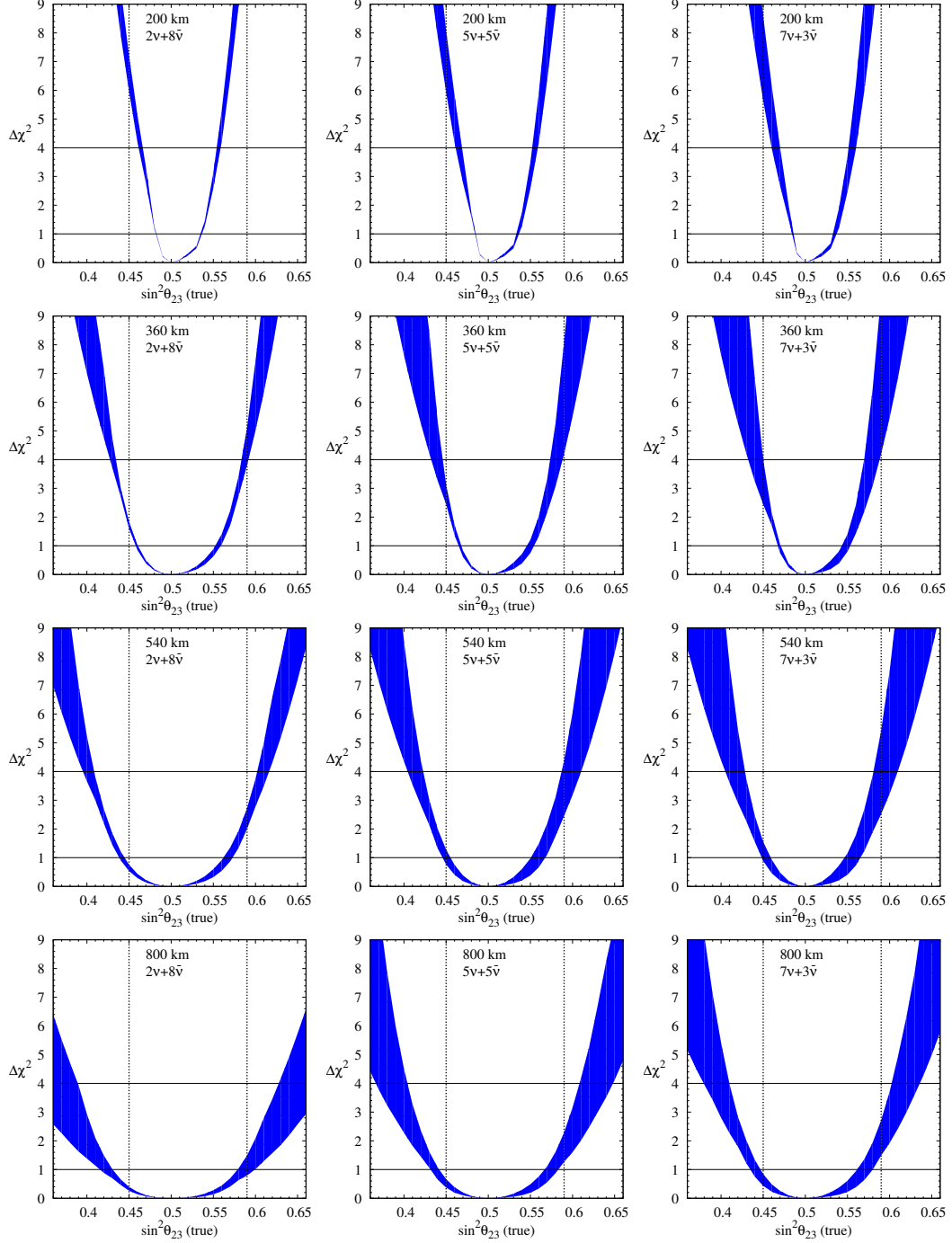


Figure 5: Octant resolution potential as a function of $\sin^2\theta_{23}(\text{true})$ for the ESS ν SB set-up. NH has been assumed as the true hierarchy. The variation in the assumed value of $\delta_{CP}(\text{true})$ leads to the formation of the band. Results corresponding to various run-plans and the assumed baseline for ESS ν SB set-up have been shown. The rows correspond to 200 km, 360 km, 540 km, and 800 km from top to bottom and the columns correspond to $2\nu + 8\bar{\nu}$, $5\nu + 5\bar{\nu}$ and $7\nu + 3\bar{\nu}$ years of running, from left to right. The horizontal black lines show 1σ and 2σ confidence level values.

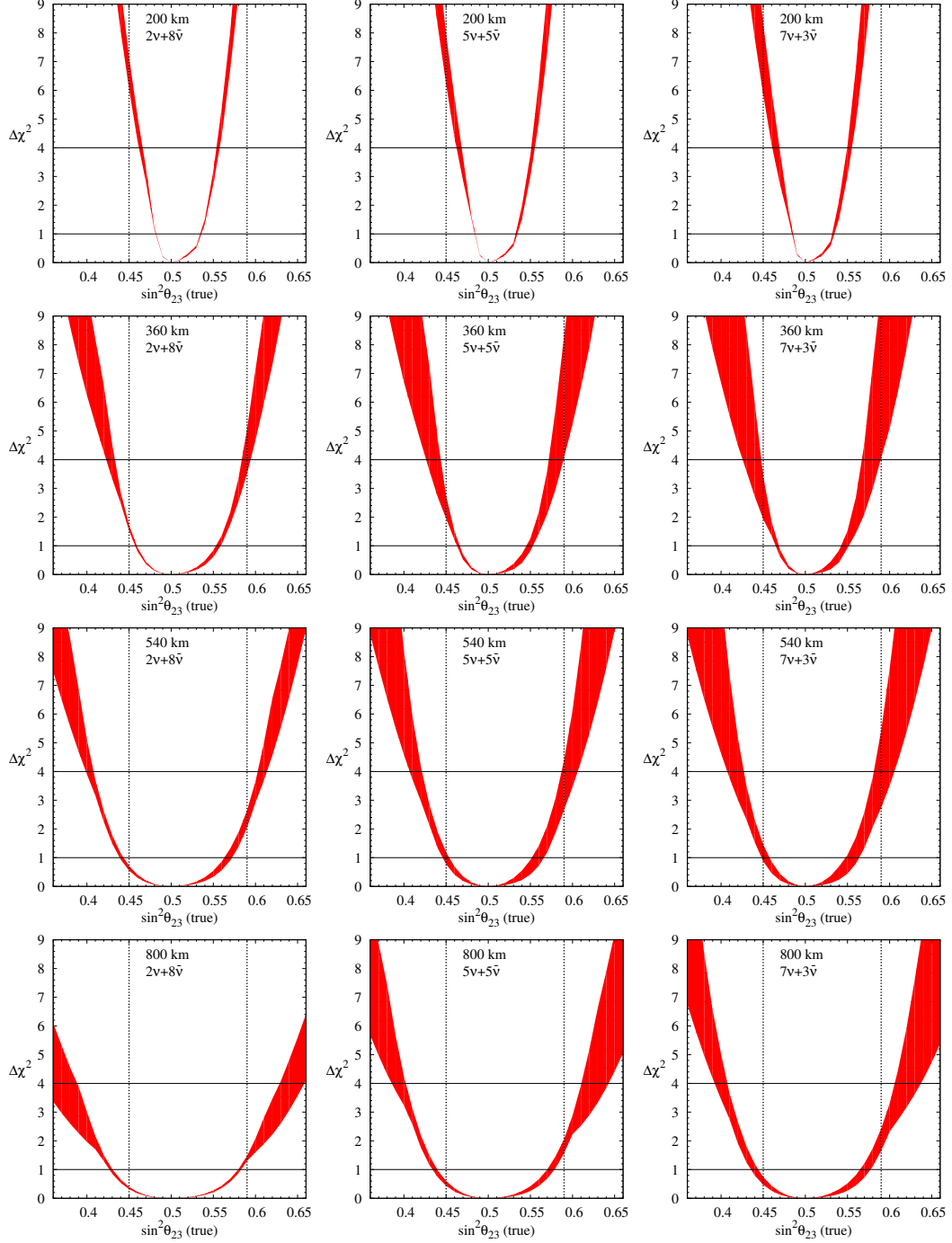


Figure 6: Octant resolution potential as a function of $\sin^2\theta_{23}(\text{true})$ for the ESS ν SB set-up. IH has been assumed as the true hierarchy. The variation in the assumed value of $\delta_{\text{CP}}(\text{true})$ leads to the formation of the band. Results corresponding to various run-plans and the assumed baseline for ESS ν SB set-up have been shown. The rows correspond to 200 km, 360 km, 540 km, and 800 km from top to bottom and the columns correspond to $2\nu + 8\bar{\nu}$, $5\nu + 5\bar{\nu}$ and $7\nu + 3\bar{\nu}$ years of running, from left to right. The horizontal black lines show 1σ and 2σ confidence level values.

200 km baseline is better-suited for the resolution of octant. Not only does it give the best octant determination potential, it also shows least $\delta_{\text{CP}} - \sin^2 \theta_{23}$ correlation. For other baselines, the contours fluctuate more depending on $\delta_{\text{CP}}(\text{true})$ as for these baselines, the ESS fluxes peak close to the second oscillation maximum, where a larger sensitivity to δ_{CP} exists. Hence, we see larger dependence of the sensitivity on the assumed true value of δ_{CP} . In particular, the performance is seen to be worst for $\delta_{\text{CP}}(\text{true}) \simeq -90^\circ$ and best for 90° .

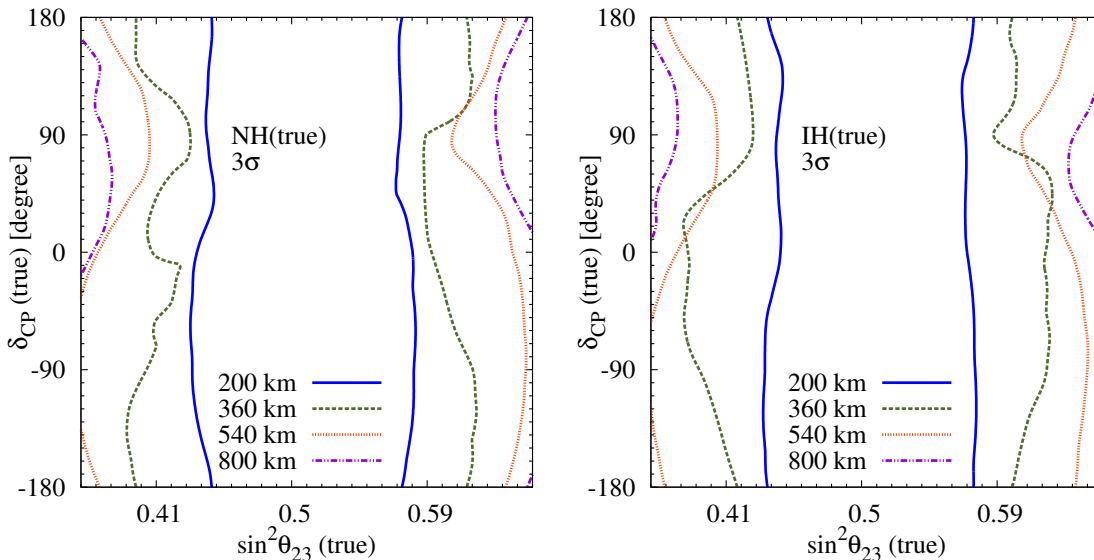


Figure 7: 3σ C.L. contours in the $\sin^2 \theta_{23}(\text{true}) - \delta_{\text{CP}}(\text{true})$ plane for the octant-resolution sensitivity of the ESS ν SB set-up. The left(right) panel corresponds to NH(IH) assumed as the true hierarchy. Results for various possible choices of baseline have been shown. The run-plan considered here is $7\nu + 3\bar{\nu}$ years of running.

5 Summary and Conclusions

The ESS proposal is envisaged as a major European facility for neutron source, to be used for both research as well as the industry. A possible promising extension of this project could be to use it simultaneously to produce a high intensity neutrino superbeam to be used for oscillation physics. Since the energy of the beam is comparatively lower, it has been proposed to do this oscillation experiment at the second oscillation maximum, for best sensitivity to CP violation discovery. In this work we have made a comparative study of all oscillation physics searches with ESS ν SB, allowing for all possible source-detector distances and with different run-plan options for running the experiment in the neutrino and anti-neutrino modes.

In particular, we have evaluated the sensitivities of the ESS ν SB proposal towards the discovery of CP violation in the lepton sector, achievable precision on atmospheric parameters, deviation of $\sin^2 \theta_{23}$ from 0.5, and finally the octant in which it lies. We have considered the prospective baselines - 200 km, 360 km, 540 km, and 800 km for the

resolution of the above mentioned unknowns. We also tested different run-plans i.e. varying combination of ν and $\bar{\nu}$ data with a total of 10 years of running. We considered $2\nu + 8\bar{\nu}$, $5\nu + 5\bar{\nu}$ and $7\nu + 3\bar{\nu}$. In the case of CP violation, we find that the best sensitivity comes for 540 km baseline where 70% coverage is possible in true δ_{CP} at 3σ while a 45% coverage is possible at 5σ . For the 200 km baseline, we find that 60% coverage is possible at 3σ and 32% coverage is possible at 5σ . We further find that all the three run-plans give the same coverage at 2σ C.L. but, at 5σ C.L., a better coverage is possible with the $7\nu + 3\bar{\nu}$ run-plan. For determination of deviation of θ_{23} from maximality, the best sensitivity is expected for the 200 km baseline with the $7\nu + 3\bar{\nu}$ run-plan, as this combination provides the largest statistics. For true $\delta_{\text{CP}} = 0$, a 3σ determination of non-maximal $\sin^2 2\theta_{23}$ can be made if true value of $\sin^2 \theta_{23} \lesssim 0.47$ or $\gtrsim 0.56$. A 5σ determination is possible if the true value of $\sin^2 \theta_{23} \lesssim 0.45$ or $\gtrsim 0.57$. In the case of octant also, we find that the 200 km baseline and $7\nu + 3\bar{\nu}$ run-plan provides the best sensitivity. We find that, assuming NH to be the true hierarchy, a 3σ resolution of octant is possible if $\sin^2 \theta_{23}(\text{true}) \lesssim 0.43$ and $\gtrsim 0.59$ for all values of $\delta_{\text{CP}}(\text{true})$. A 5σ determination could be possible if $\sin^2 \theta_{23}(\text{true}) \lesssim 0.37$ and $\gtrsim 0.63$.

Finally, we end this paper with a comparison of the deviation from maximality and octant of θ_{23} discovery reach of the ESS ν SB set-up with the other next-generation proposed long baseline superbeam experiments. We show in Fig. 8 this comparison for the ESS ν SB set-up with the 200 km baseline option and $7\nu + 3\bar{\nu}$ run-plan (green short dashed lines), LBNE with 10 kt liquid argon detector (orange dotted lines), and LBNO with 10 kt liquid argon detector (purple dot-dashed lines). For LBNE and LBNO, we have used the experimental specifications as given in [70]. In generating the plots for these three future facilities, we have added the projected data from T2K ($2.5\nu + 2.5\bar{\nu}$) and NO ν A ($3\nu + 3\bar{\nu}$). The details of these experiments are the same as considered in [53]. The left hand panel of this figure shows the $\Delta\chi^2$ as a function of $\sin^2 \theta_{23}(\text{true})$ for deviation of θ_{23} from its maximal value for $\delta_{\text{CP}}(\text{true}) = 0$. The ESS ν SB set-up is seen to perform better than the other two superbeam options, mainly due to larger statistics. With larger detectors, both LBNE and LBNO will start to be competitive. The right hand panel shows 5σ contours for the octant of θ_{23} discovery reach in the $\delta_{\text{CP}}(\text{true})$ - $\sin^2 \theta_{23}(\text{true})$ plane. The three experiments are very comparable, with the best reach coming for the ESS ν SB set-up with the 200 km baseline option and $7\nu + 3\bar{\nu}$ run-plan.

To conclude, among all four choices of the baselines, the best results for sensitivity to deviation from maximality and resolution of octant is expected for the 200 km baseline option. On the other hand, chances for discovery of CP violation are best for the 540 km baseline, which sits on the second oscillation maximum and hence gives the maximum coverage in true δ_{CP} . However, the CP violation discovery prospects for the 200 km baseline is only slightly worse. We have also seen that for all oscillation physics results, the $7\nu + 3\bar{\nu}$ run-plan provides the best sensitivity amongst the three run-plan choices considered. While we appreciate the merit of putting the detector at the second oscillation peak, this paper shows the advantage of another baseline option, in particular, 200 km.

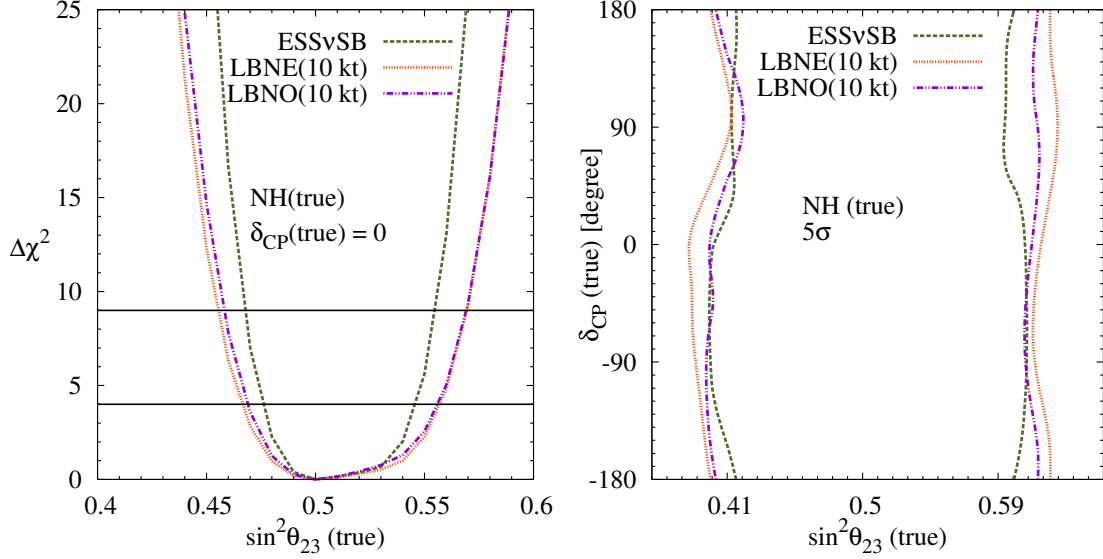


Figure 8: A comparison of the future facilities LBNE and LBNO with the ESS ν SB set-up. **Left panel: non-maximal θ_{23} discovery potential. Right panel: octant resolution potential.** For ESS ν SB, a 200 km long baseline and a $7\nu + 3\bar{\nu}$ running is considered. For both LBNE and LBNO, a 10 kt LArTPC detector and a $5\nu + 5\bar{\nu}$ running is considered. The horizontal black lines show 2σ and 3σ C.L.

Acknowledgments

We thank E. Fernandez-Martinez, L. Agostino, and T. Ekelöf for useful discussions. S.K.A acknowledges the support from DST/INSPIRE Research Grant [IFA-PH-12], Department of Science and Technology, India. S.C. and S.P. acknowledge support from the Neutrino Project under the XII plan of Harish-Chandra Research Institute. S.C. acknowledges partial support from the European Union FP7 ITN INVISIBLES (Marie Curie Actions, PITN-GA-2011-289442).

References

- [1] K. Olive et al. (Particle Data Group), *Chin.Phys.* **C38**, 090001 (2014).
- [2] B. Cleveland, T. Daily, J. Davis, Raymond, J. R. Distel, K. Lande, et al., *Astrophys.J.* **496**, 505 (1998).
- [3] M. Altmann et al. (GNO COLLABORATION), *Phys.Lett.* **B616**, 174 (2005), [hep-ex/0504037](#).
- [4] J. Hosaka et al. (Super-Kamkiokande Collaboration), *Phys.Rev.* **D73**, 112001 (2006), [hep-ex/0508053](#).
- [5] Q. Ahmad et al. (SNO Collaboration), *Phys.Rev.Lett.* **89**, 011301 (2002), [nucl-ex/0204008](#).
- [6] B. Aharmim et al. (SNO Collaboration), *Phys.Rev.Lett.* **101**, 111301 (2008), [0806.0989](#).
- [7] B. Aharmim et al. (SNO Collaboration), *Phys.Rev.* **C81**, 055504 (2010), [0910.2984](#).
- [8] C. Arpesella et al. (The Borexino Collaboration), *Phys.Rev.Lett.* **101**, 091302 (2008), [0805.3843](#).

- [9] Y. Fukuda et al. (Super-Kamiokande Collaboration), Phys.Rev.Lett. **81**, 1562 (1998), [hep-ex/9807003](#).
- [10] Y. Ashie et al. (Super-Kamiokande Collaboration), Phys.Rev. **D71**, 112005 (2005), [hep-ex/0501064](#).
- [11] T. Araki et al. (KamLAND Collaboration), Phys.Rev.Lett. **94**, 081801 (2005), [hep-ex/0406035](#).
- [12] S. Abe et al. (KamLAND Collaboration), Phys.Rev.Lett. **100**, 221803 (2008), [0801.4589](#).
- [13] F. An et al. (Daya Bay), Phys.Rev.Lett. **108**, 171803 (2012), [1203.1669](#).
- [14] F. An et al. (Daya Bay), Chin. Phys. **C37**, 011001 (2013), [1210.6327](#).
- [15] J. Ahn et al. (RENO), Phys.Rev.Lett. **108**, 191802 (2012), [1204.0626](#).
- [16] Y. Abe et al. (Double Chooz), Phys.Rev.Lett. **108**, 131801 (2012), [1112.6353](#).
- [17] Y. Abe et al. (Double Chooz), Phys.Rev. **D86**, 052008 (2012), [1207.6632](#).
- [18] M. Ahn et al. (K2K Collaboration), Phys.Rev. **D74**, 072003 (2006), [hep-ex/0606032](#).
- [19] P. Adamson et al. (MINOS Collaboration), Phys.Rev.Lett. **101**, 131802 (2008), [0806.2237](#).
- [20] P. Adamson et al. (MINOS Collaboration), Phys.Rev.Lett. **107**, 181802 (2011), [1108.0015](#).
- [21] P. Adamson et al. (MINOS), Phys.Rev.Lett. (2013), [1301.4581](#).
- [22] K. Abe et al. (T2K Collaboration), Phys.Rev.Lett. **107**, 041801 (2011), [1106.2822](#).
- [23] K. Abe et al. (T2K) (2013), [1304.0841](#).
- [24] B. Pontecorvo, Sov.Phys.JETP **26**, 984 (1968).
- [25] V. Gribov and B. Pontecorvo, Phys.Lett. **B28**, 493 (1969).
- [26] S. M. Bilenky (2014), [1408.2864](#).
- [27] F. An et al. (Daya Bay Collaboration) (2013), [1310.6732](#).
- [28] E. K. Akhmedov, Nucl.Phys. **B538**, 25 (1999), [hep-ph/9805272](#).
- [29] E. K. Akhmedov, A. Dighe, P. Lipari, and A. Smirnov, Nucl.Phys. **B542**, 3 (1999), [hep-ph/9808270](#).
- [30] M. Chizhov and S. Petcov, Phys.Rev.Lett. **83**, 1096 (1999), [hep-ph/9903399](#).
- [31] M. Banuls, G. Barenboim, and J. Bernabeu, Phys.Lett. **B513**, 391 (2001), [hep-ph/0102184](#).
- [32] R. Gandhi, P. Ghoshal, S. Goswami, P. Mehta, and S. U. Sankar, Phys.Rev.Lett. **94**, 051801 (2005), [hep-ph/0408361](#).
- [33] V. Barger, R. Gandhi, P. Ghoshal, S. Goswami, D. Marfatia, et al., Phys.Rev.Lett. **109**, 091801 (2012), [1203.6012](#).
- [34] S. Pascoli and T. Schwetz, Adv.High Energy Phys. **2013**, 503401 (2013).
- [35] M. Blennow, P. Coloma, P. Huber, and T. Schwetz, JHEP **1403**, 028 (2014), [1311.1822](#).
- [36] S. Agarwalla et al. (LAGUNA-LBNO Collaboration) (2013), [1312.6520](#).
- [37] S. K. Agarwalla, Adv.High Energy Phys. **2014**, 457803 (2014), [1401.4705](#).
- [38] Y.-F. Li, Int.J.Mod.Phys.Conf.Ser. **31**, 1460300 (2014), [1402.6143](#).

- [39] RENO-50 collaboration (RENO-50), in *International Workshop on RENO-50 toward Neutrino Mass Hierarchy* (2013), URL <http://home.kias.re.kr/MKG/h/reno50/>.
- [40] S. Antusch, P. Huber, J. Kersten, T. Schwetz, and W. Winter, *Phys.Rev.* **D70**, 097302 (2004), [hep-ph/0404268](#).
- [41] H. Minakata, M. Sonoyama, and H. Sugiyama, *Phys.Rev.* **D70**, 113012 (2004), [hep-ph/0406073](#).
- [42] M. Gonzalez-Garcia, M. Maltoni, and A. Y. Smirnov, *Phys.Rev.* **D70**, 093005 (2004), [hep-ph/0408170](#).
- [43] D. Choudhury and A. Datta, *JHEP* **0507**, 058 (2005), [hep-ph/0410266](#).
- [44] S. Choubey and P. Roy, *Phys.Rev.* **D73**, 013006 (2006), [hep-ph/0509197](#).
- [45] D. Indumathi, M. Murthy, G. Rajasekaran, and N. Sinha, *Phys.Rev.* **D74**, 053004 (2006), [hep-ph/0603264](#).
- [46] T. Kajita, H. Minakata, S. Nakayama, and H. Nunokawa, *Phys.Rev.* **D75**, 013006 (2007), [hep-ph/0609286](#).
- [47] K. Hagiwara and N. Okamura, *JHEP* **0801**, 022 (2008), [hep-ph/0611058](#).
- [48] A. Samanta and A. Smirnov, *JHEP* **1107**, 048 (2011), [1012.0360](#).
- [49] S. Choubey and A. Ghosh, *JHEP* **1311**, 166 (2013), [1309.5760](#).
- [50] A. Chatterjee, P. Ghoshal, S. Goswami, and S. K. Raut, *JHEP* **1306**, 010 (2013), [1302.1370](#).
- [51] S. K. Agarwalla, S. Prakash, and S. U. Sankar, *JHEP* **1307**, 131 (2013), [1301.2574](#).
- [52] P. Huber, M. Lindner, T. Schwetz, and W. Winter, *JHEP* **0911**, 044 (2009), [0907.1896](#).
- [53] S. K. Agarwalla, S. Prakash, S. K. Raut, and S. U. Sankar, *JHEP* **1212**, 075 (2012), [1208.3644](#).
- [54] P. Machado, H. Minakata, H. Nunokawa, and R. Z. Funchal (2013), [1307.3248](#).
- [55] M. Ghosh, P. Ghoshal, S. Goswami, and S. K. Raut (2014), [1401.7243](#).
- [56] K. Dick, M. Freund, M. Lindner, and A. Romanino, *Nucl.Phys.* **B562**, 29 (1999), [hep-ph/9903308](#).
- [57] A. Donini, M. Gavela, P. Hernandez, and S. Rigolin, *Nucl.Phys.* **B574**, 23 (2000), [hep-ph/9909254](#).
- [58] H. Minakata, *Nucl.Phys.Proc.Suppl.* **235-236**, 173 (2013), [1209.1690](#).
- [59] E. Baussan, M. Dracos, T. Ekelof, E. F. Martinez, H. Ohman, et al. (2012), [1212.5048](#).
- [60] E. Baussan et al. (ESSnuSB Collaboration) (2013), [1309.7022](#).
- [61] L. Agostino et al. (MEMPHYS Collaboration), *JCAP* **1301**, 024 (2013), [1206.6665](#).
- [62] J.-E. Campagne, M. Maltoni, M. Mezzetto, and T. Schwetz, *JHEP* **0704**, 003 (2007), [hep-ph/0603172](#).
- [63] P. Adamson et al. (MINOS Collaboration), *Phys.Rev.Lett.* (2014), [1403.0867](#).
- [64] A. Himmel (Collaboration for the Super-Kamiokande) (2013), [1310.6677](#).
- [65] K. Abe et al. (T2K Collaboration), *Phys.Rev.Lett.* **112**, 181801 (2014), [1403.1532](#).
- [66] F. Capozzi, G. Fogli, E. Lisi, A. Marrone, D. Montanino, et al. (2013), [1312.2878](#).

- [67] D. Forero, M. Tortola, and J. Valle (2014), [1405.7540](#).
- [68] H. Minakata, H. Sugiyama, O. Yasuda, K. Inoue, and F. Suekane, Phys.Rev. **D68**, 033017 (2003), [hep-ph/0211111](#).
- [69] K. Hiraide, H. Minakata, T. Nakaya, H. Nunokawa, H. Sugiyama, et al., Phys.Rev. **D73**, 093008 (2006), [hep-ph/0601258](#).
- [70] S. K. Agarwalla, S. Prakash, and S. Uma Sankar, JHEP **1403**, 087 (2014), [1304.3251](#).
- [71] V. Barger, A. Bhattacharya, A. Chatterjee, R. Gandhi, D. Marfatia, et al., Phys.Rev. **D89**, 011302 (2014), [1307.2519](#).
- [72] V. Barger, A. Bhattacharya, A. Chatterjee, R. Gandhi, D. Marfatia, et al. (2014), [1405.1054](#).
- [73] M. Ghosh, P. Ghoshal, S. Goswami, and S. K. Raut, JHEP **1403**, 094 (2014), [1308.5979](#).
- [74] P. Huber, M. Lindner, and W. Winter, Comput.Phys.Commun. **167**, 195 (2005), [hep-ph/0407333](#).
- [75] P. Huber, J. Kopp, M. Lindner, M. Rolinec, and W. Winter, Comput.Phys.Commun. **177**, 432 (2007), [hep-ph/0701187](#).
- [76] Enrique Fernandez Martinez, private communication (2013).
- [77] Luca Agostino, private communication (2013).
- [78] P. Coloma and E. Fernandez-Martinez, JHEP **1204**, 089 (2012), [1110.4583](#).
- [79] L. Wolfenstein, Phys. Rev. **D17**, 2369 (1978).
- [80] M. Freund, Phys.Rev. **D64**, 053003 (2001), [hep-ph/0103300](#).
- [81] E. K. Akhmedov, R. Johansson, M. Lindner, T. Ohlsson, and T. Schwetz, JHEP **0404**, 078 (2004), [hep-ph/0402175](#).
- [82] A. Cervera et al., Nucl. Phys. **B579**, 17 (2000), [Erratum-ibid.B593:731-732,2001], [hep-ph/0002108](#).
- [83] H. Nunokawa, S. J. Parke, and R. Zukanovich Funchal, Phys.Rev. **D72**, 013009 (2005), [hep-ph/0503283](#).
- [84] A. de Gouvea, J. Jenkins, and B. Kayser, Phys.Rev. **D71**, 113009 (2005), [hep-ph/0503079](#).
- [85] G. Fogli, E. Lisi, A. Marrone, D. Montanino, A. Palazzo, et al., Phys.Rev. **D67**, 073002 (2003), [hep-ph/0212127](#).
- [86] P. Huber, M. Lindner, and W. Winter, Nucl. Phys. **B645**, 3 (2002), [hep-ph/0204352](#).
- [87] X. Qian (Daya Bay) (2012), talk given at the NuFact 2012 Conference, July 23-28, 2012, Williamsburg, USA, <http://www.jlab.org/conferences/nufact12/>.
- [88] K. Abe, T. Abe, H. Aihara, Y. Fukuda, Y. Hayato, et al. (2011), [1109.3262](#).
- [89] S. K. Agarwalla, S. Prakash, and W. Wang (2013), [1312.1477](#).
- [90] S. K. Raut, Mod.Phys.Lett. **A28**, 1350093 (2013), [1209.5658](#).